

A Multi-scale Model for Mass Transport in Arteries and Tissue

T. Köppl, R. Helmig, and B. Wohlmuth

Abstract In this paper, we are concerned with the simulation of blood flow and mass transport in vascularized human tissue. Our mathematical model is based on a domain decomposition approach, i.e., we separate the blood vessel network from the tissue and assign different flow and transport models to them. In a second step, the different models are coupled in a weakly consistent way. Flow and transport processes within a 3D tissue are governed by standard equations for porous media flow while within the larger blood vessels less complex 1D models can be used, and the smaller blood vessels can be even treated by 0D lumped parameter models. This results in a 3D-1D-0D coupled multi-scale model. By means of this tri-directionally coupled system, the influence of a peripheral stenosis on tissue perfusion and oxygen supply is investigated.

1 Introduction

Mathematical models have become more and more important in many applications from medicine and biology [5, 6, 8, 10]. In this paper, we are concerned with the simulation of blood flow and mass transport, e.g. oxygen transport, from the heart through the arterial vessel system to the peripheral vessels and tissue. In particular, the impact of peripheral arterial stenoses on blood flow and oxygen supply is investigated. A stenosis is an abnormal narrowing in a blood vessel. Such a narrowing may arise from atherosclerosis, a specific form of arteriosclerosis, which is caused by the accumulation of fatty plaques and cholesterol. Typically, it appears in large- or middle-sized arteries. A stenosis causes pressure drops and reduced oxygen supply,

T. Köppl (✉) • R. Helmig

Department of Hydromechanics and Modelling of Hydrosystems, Pfaffenwaldring 61, D-70569 Stuttgart, Germany

e-mail: tobias.koepl@iws.uni-stuttgart.de; rainer.helmig@iws.uni-stuttgart.de

B. Wohlmuth

Institute for Numerical Mathematics, Technische Universität München, Boltzmannstr. 3, D-85748 Garching b. München, Germany

e-mail: wohlmuth@ma.tum.de

© Springer International Publishing Switzerland 2015

M. Mehl et al. (eds.), *Recent Trends in Computational Engineering - CE2014*,

Lecture Notes in Computational Science and Engineering 105,

DOI 10.1007/978-3-319-22997-3_12

ischemia in the distal tissue results. If a stenosis is located in the distal part of an arm or a leg, it is called peripheral stenosis [18]. “Distal” is a term used in anatomy to describe parts of a feature that are respectively distant from a certain reference point. The counterpart is the term “proximal” describing parts of a feature that are close to a certain reference point. For our model we use the heart as a reference point.

Modeling blood flow and transport processes from large vessels down to the capillaries is a very complex matter, since one has to simulate flow on different scales through a huge number of vessels. To resolve every vessel within the arterial tree is unaffordable in terms of numerical simulation. Therefore, we take only the most important arteries of the vessel system into account, i.e., we truncate the network after some bifurcations. In the larger vessels the flow is fast compared with the flow in the arterioles and the rather diffusion-dominated flow in the capillaries and tissue. Because of this heterogeneous flow behavior, we require for the numerical modeling a scheme that uses small time steps for the fast flow region and large time steps for the slow flow region. In order to keep the computational costs low, it is necessary to establish for the network flow a model which causes low computational effort in each time step. In this context, 1D reduced models proved very effective [4, 6, 9, 10].

To determine flow and transport through a whole network, a *domain decomposition approach* has been applied, i.e., the network is split into its single vessels and the reduced 1D models are assigned to each vessel. At each bifurcation, the adjacent 1D models are coupled by an algebraic system of equations. The resistance and compliance of the omitted vessels are accounted for by lumped parameter models [1] which are given by a system of ordinary differential equations (ODEs, 0D models). The influence of a stenosis is also simulated by lumped parameter models presented in [20].

Flow and transport processes from the blood vessels into the surrounding tissue are modeled with the help of the coupling strategies presented in [6, 7]. In these publications, human tissue and the feeding capillaries are regarded as a 3D porous medium. Within the porous medium, flow and transport are governed by a diffusion-reaction equation, Darcy’s law and a convection-diffusion equation.

The paper is structured as follows: In Sect. 2, we present some mathematical models governing the flow and transport processes in the vessels and tissue. Furthermore, we explain in detail, how the network and tissue models are coupled. In the following section (Sect. 3) a short description of the numerical discretization can be found. Our simulation results are discussed in Sect. 4. Finally, we make some concluding remarks (Sect. 5).

2 Mathematical Model

For our numerical simulations we consider an arterial network presented in [19, 22]. It consists of the 55 main arteries of the human blood vessel system. In order to model a peripheral stenosis, we place a stenosis in the middle of artery 54 (posterior

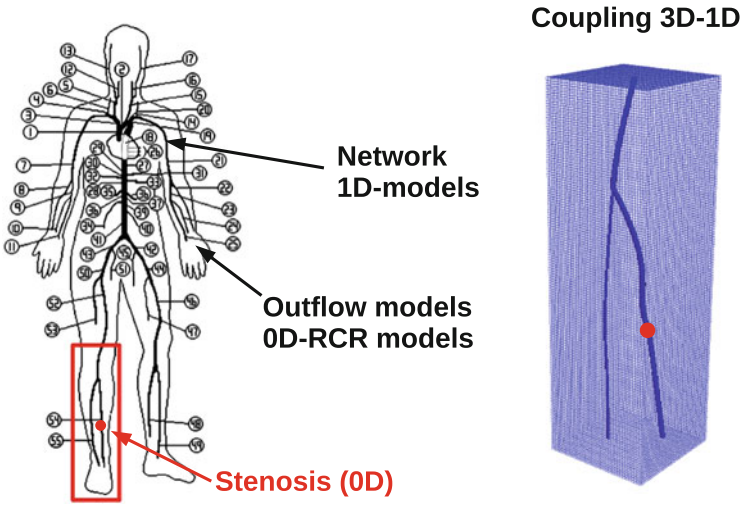


Fig. 1 Arterial network consisting of 55 large and middle sized arteries. In artery 54 a stenosis is placed to simulate the influence of reduced blood flow and oxygen transport on distal tissue [22] (left). The small arteries, capillaries and tissue in the red rectangle are considered as a porous medium and put together with the larger arteries in a cuboid (right). Flow and transport within the arterial tree and the porous medium are governed by a 3D-1D-0D coupled multi-scale model

tibial artery, see Fig. 1, left). Since only the local impact of the stenosis on tissue perfusion is of interest, not the entire network is embedded into tissue, but only artery 54, 55 and the distal third of artery 53 are coupled with the surrounding tissue (red rectangle in Fig. 1, left). These vessels or vessel parts form a subnetwork S_N consisting of four vessels V_1, V_2, V_3 and V_4 . By V_1 we denote the distal third of artery 53, by V_2 the proximal part of artery 54. V_3 indicates the distal part of artery 54 and V_4 is identical with artery 55 (see Fig. 2, left). In the following, we present some models for the arterial network flow and transport, the stenosis and the coupling of flow and transport in the tissue with the subnetwork S_N .

2.1 Model for Arterial Network Flow and Transport

In this subsection, we give a description of the domain decomposition approach providing the basis for our network model.

2.1.1 Flow and Transport Through a Single Vessel

The non-linear 1D system of transport equations for the i -th arterial vessel having the length l_i [cm] and the section area $A_{0,i}$ [cm²] is given by Alastruey et al. [1] and

D'Angelo [6, Chap. 2].

$$\frac{\partial A_i}{\partial t} + \frac{\partial Q_i}{\partial z} = \phi_A, \quad z \in (0, l_i), \quad t > 0, \quad (1)$$

$$\frac{\partial Q_i}{\partial t} + \frac{\partial}{\partial z} \left(\frac{Q_i^2}{A_i} \right) + \frac{A_i}{\rho} \frac{\partial p_i}{\partial z} = -K_r \frac{Q_i}{A_i}, \quad z \in (0, l_i), \quad t > 0, \quad (2)$$

$$\frac{\partial \Gamma_i}{\partial t} + \frac{\partial}{\partial z} \left(\frac{\Gamma_i Q_i}{A_i} \right) = \theta_C, \quad z \in (0, l_i), \quad t > 0, \quad (3)$$

where A_i , Q_i , Γ_i and p_i denote the section area, average volumetric flux, averaged concentration and mean pressure of the i -th vessel, $i \in \{1, \dots, 55\}$, respectively. ρ is the blood density. The coefficient K_r is a resistance parameter linked to the blood viscosity η : $K_r = \frac{22\pi\eta}{\rho}$. ϕ_A and θ_C will be specified in Sect. 2.2.1.

If $G_{0,i}$ and $A_{0,i}$ are constant along z , a suitable way to close this system is to provide an algebraic relation between the pressure and the vessel area A_i :

$$p_i(z, t) = G_{0,i} \left(\sqrt{\frac{A_i}{A_{0,i}}} - 1 \right), \quad G_{0,i} = \frac{\sqrt{\pi} h_{0,i} E_i}{(1 - \nu^2) \sqrt{A_{0,i}}}, \quad (4)$$

where E_i is the Young modulus, $h_{0,i}$ is the vessel thickness and ν is the Poisson ratio. An analysis of the characteristics of system (1)–(4), reveals that changes in pressure, flow rate and concentration are propagated by $W_{1,i}$, $W_{2,i}$ and $W_{3,i}$ [6, Chap. 2]:

$$W_{1,i} = -\frac{Q_i}{A_i} + 4\sqrt{\frac{G_{0,i}}{2\rho}} \left(\frac{A_i}{A_{0,i}} \right)^{\frac{1}{4}}, \quad W_{2,i} = \frac{Q_i}{A_i} + 4\sqrt{\frac{G_{0,i}}{2\rho}} \left(\frac{A_i}{A_{0,i}} \right)^{\frac{1}{4}}, \quad W_{3,i} = \frac{\Gamma_i}{A_i}, \quad (5)$$

where under physiological conditions, it can be shown that $W_{1,i}$ is a backward and $W_{2,i}$ is a forward traveling wave. The propagation of $W_{3,i}$ depends on the sign of Q_i .

2.1.2 Bifurcations

At a bifurcation the adjacent 1D models are coupled by an algebraic system of equations providing for each time step the missing boundary conditions. Every subsystem requires three boundary values. Therefore nine equations have to be established. The first three equations are obtained from the characteristics which leave the vessels. According to the previous subsection there is for the AQ -variables at least one outgoing characteristic at each boundary. Three further

equations are derived from mass conservation and the continuity of the total pressure p_t .

$$p_t = \frac{1}{2}\rho \left(\frac{Q_i}{A_i}\right)^2 + G_{0,i} \left(\sqrt{\frac{A_i}{A_{0,i}}} - 1\right). \quad (6)$$

These six equations form a subsystem for the flow variables A and Q [19, 22]. In order to obtain the boundary values for the concentration variable Γ one has to check first, how many values can be determined by standard upwinding. Depending on that, the system is closed by the continuity of the volumetric concentration $C_v = \Gamma/A$ or a conservation equation. For a detailed discussion of this system of equations we refer to [14].

2.1.3 Outflow Boundaries

Since we model only a small part of the arterial vessel system by the 1D model (1)–(4), we have to provide at the outflow boundaries of the network boundary conditions accounting for the hemodynamic effects of the omitted arteries and veins. In this context 0D lumped parameter models proved to be very effective. They are given by a system of ODEs having the pressure and the flow rate as solution variables.

The ODE system exhibits three parameters R , C and L . R models the resistance of the omitted vessels, C is the compliance and L incorporates the inductive effects. By means of this model one can compute the ingoing characteristic. Combined with the outgoing characteristic and (4) the boundary values for the flow variables A and Q can be determined. The values for R and C can be found, e.g., in [20]. The concentration values Γ are computed by standard upwinding, if blood is leaving the vessel. Otherwise a boundary value has to be provided externally, e.g., the average concentration of oxygen in blood: $C_{O_2} = 8.75 \mu\text{mol}/\text{cm}^3$. Details about this model can be found in [1, 15].

2.1.4 Inflow Boundary

Within the considered network (see Fig. 1) we have only a single inflow boundary at the inlet of the aorta (Vessel 1). In order to model the pulsure of the adjacent heart, we prescribe the following flow rate profile:

$$Q(t) = \begin{cases} 485 \cdot \sin\left(\frac{\pi}{T}t\right) \frac{\text{cm}^3}{\text{s}} & \text{for } 0.0 \text{ s} \leq t \leq T, \\ 0 \frac{\text{cm}^3}{\text{s}} & \text{for } T < t \leq 1.0 \text{ s}. \end{cases} \quad (7)$$

For $t > 1$ it holds: $Q(t) = Q(t + 1)$. In medical research, the time period $[0.0, T]$ is referred to as *systole*, while the time period $(T, 1.0]$ is known as *diastole*. For our simulations, we choose $T = 0.3$ s. Integrating the function in (7) over 1 min yields that 5.5577 l are leaving the heart within 1 min. This is in agreement with medical literature [3]. Together with the outgoing characteristic $W_{1,1}$ the boundary value for the section area A_1 can be computed. For the concentration we prescribe the constant C_{O_2} : $C_{O_2} = \Gamma_1(0, t)/A_1(0, t)$.

2.1.5 Stenosis

The 1D model (1)–(4) can not treat vessels with varying section areas $A_{0,i}$ [9]. Therefore the stenosis model described in [20] was incorporated, where the flow rate q_s and the pressure p_s within the stenosis are governed by:

$$C_s \frac{\partial p_s}{\partial t} = Q_{in} - Q_{out}, \quad (8)$$

$$-\frac{K_u \rho l_s}{A_0} \frac{\partial q_s}{\partial t} = \Delta p_s + \frac{K_v \eta}{A_0 D_0} q_s + \frac{K_t \rho}{2A_0^2} \left(\frac{A_0}{A_s} - 1 \right)^2 q_s |q_s|. \quad (9)$$

Q_{in} and Q_{out} are the flow rates at the inlet and the outlet of the stenosis. The pressure drop $\Delta p_s = p_{out} - p_{in}$ is the difference of the pressures at the outlet and the inlet. Using (4), the values Q_{in} , Q_{out} , p_{in} and p_{out} are provided by the adjacent 1D models. C_s is the compliance of the stenosis and l_s denotes its length. In this paper, we choose $l_s = 3.0$ cm. A_0 and A_s define the section areas of the normal and stenotic segments. D_0 and D_s are the corresponding diameters. Further, K_u , K_v and K_t are empirical parameters: $K_u = 1.20$, $K_v = 32.0 \cdot (0.83 \cdot l_s + 1.64 \cdot D_s) \cdot (A_0/A_s)^2 / D_0$ and $K_t = 1.52$.

The ODEs (8) and (9) yield together with (4) two boundary conditions for the flow variables. The missing conditions are again derived from the outgoing characteristics. The concentration variables are obtained by standard upwinding and the continuity of the volumetric oxygen concentration C_v . For further information, we refer to [15].

2.2 Model for Tissue Flow and Transport

Human tissue can be regarded as an accumulation of cells having a specific task. However, the cells do not cover the whole tissue volume, between the cells space saturated with blood can occur, e.g., due to feeding capillaries. For that reason it is common practice to model flow and transport processes in the tissue by PDEs governing porous media flow and transport [13, 21]. In this section we outline how

the PDEs for porous media flow and transport can be coupled with the reduced 1D models described in the previous section.

Let us denote the 3D porous tissue matrix by $\Omega \subset \mathbb{R}^3$. The unknowns associated with the 3D problems are indicated by u_{3d} , $u \in \{p, c\}$. p [kPa] stands for the pressure variable and c [mmol/cm³] for the volumetric concentration.

The main axes of the vessels V_1 – V_4 belonging to the subnetwork S_N in Ω are given by curves Λ_i , $i \in \{1, 2, 3, 4\}$ and are parameterized as follows:

$$\Lambda_i : [0, l_i] \rightarrow \Omega, \quad s \mapsto \mathbf{x}_{c_i}(s).$$

l_i is the length of vessel V_i . By this, the corresponding 1D models are linked to their position within Ω . Combining the curves Λ_i yields a 1D representation Λ of the embedded subnetwork S_N : $\Lambda = \bigcup_{i=1}^4 \Lambda_i$.

2.2.1 Tissue Perfusion Problem

The pressure p_{3d} is governed by the following parabolic PDE [6, Chap. 6.3]:

$$C_{3d} \frac{\partial}{\partial t} p_{3d} - \nabla \circ (K_{3d} \nabla p_{3d}) + \alpha p_{3d} - \phi_{3d} = f_p. \quad (10)$$

The parameter C_{3d} [kPa⁻¹] denotes the hydraulic compliance of the tissue. K_{3d} [cm² kPa⁻¹ s⁻¹] is the tissue permeability for blood, α [kPa⁻¹ s⁻¹] is the hydraulic conductance and the source term f_p is given by:

$$f_p = \alpha p_{ven} + \frac{q_{out}(t)}{Vol}, \quad t \geq 0, \quad (11)$$

where p_{ven} is the average venous blood pressure, Vol is the volume perfused by the outlets of vessel V_3 and V_4 . $q_{out}(t)$ is the sum of the flow rates Q_3^{out} and Q_4^{out} at the outlets of vessel V_3 and V_4 :

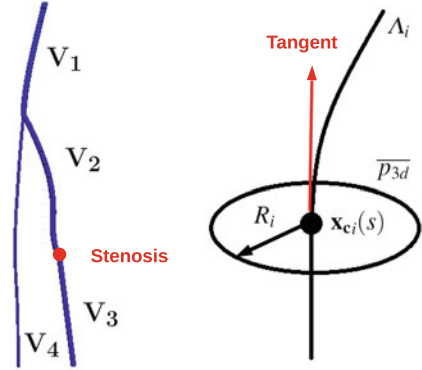
$$q_{out}(t) = Q_3^{out}(t) \delta_{\Lambda_3(l_3)} + Q_4^{out}(t) \delta_{\Lambda_4(l_4)}.$$

$\delta_{\Lambda_i(l_i)}$ is a Dirac measure concentrated on the point $\Lambda_i(l_i) \in \Omega$.

By ϕ_{3d} we denote an exchange term. It accounts for the blood transfer from the vessels V_i caused by smaller arteries branching out of them to supply the surrounding tissue. To decide how much blood volume is leaving V_i , we compare for every curve parameter s the 1D pressure $p_i(s)$ with an averaged pressure $p_{3d}(s)$.

For the computation of this average, one has to integrate p_{3d} on a circle of radius $R_i = \sqrt{A_i/\pi}$ with center $\mathbf{x}_{c_i}(s)$ and perpendicular to the tangent in $\mathbf{x}_{c_i}(s)$ (see Fig. 2, right).

Fig. 2 Decomposition of the subnetwork S_N embedded in the tissue block. The vessel containing the stenosis is split into two parts. By V_i , $i \in \{1, 2, 3, 4\}$ we denote the corresponding vessels (*left*). Computation of an averaged pressure value $\overline{p_{3d}}$ concerning a circle of radius R_i around the curve point $x_{c,i}$ and perpendicular to the tangent in $x_{c,i}$ (*right*)



By means of this average, we define a source term ϕ given by the difference of p_i and $\overline{p_{3d}}$. The source term is weighted by the proportionality factor $L_{p,i}$ [$\text{cm kPa}^{-1} \text{s}^{-1}$] to account for the number of arteries that are branching out of V_i :

$$\phi(p_{3d}, p_i)(s) = 2\pi R_i L_{p,i} \left(p_i(s) - \overline{p_{3d}(s)} \right),$$

$$\overline{p_{3d}(s)} = \int_0^1 p_{3d}(s, R_i, 2\pi\theta) d\theta, \text{ if } s \in [0, l_i], i \in \{1, \dots, 4\}. \quad (12)$$

To embed this quantity into the 3D problem, the source term ϕ is used as a weighting factor for a Dirac measure δ_{Λ_i} concentrated on the main axis of vessel V_i . All in all we have for the exchange term ϕ_{3d} :

$$\phi_{3d}(s) = \phi(p_{3d}, p_i)(s) \delta_{\Lambda_i}, \text{ if } s \in [0, l_i], i \in \{1, \dots, 4\}.$$

The source term ϕ_A for the vessels V_i in (1) is: $\phi_A = -\phi(p_{3d}, p_i)$ and θ_C in (3) is given by:

$$\theta_C(s) = -\phi(p_{3d}, p_i) \frac{\Gamma_i}{A_i}(s), \text{ if } s \in [0, l_i], i \in \{1, \dots, 4\}.$$

For the remaining vessels which do not belong to S_N , we set: $\phi_A \equiv 0$ and $\theta_C \equiv 0$.

2.2.2 Transport Problem

The transport problem for oxygen concentration in tissue is given by [6, Chap. 6.3]:

$$\frac{\partial}{\partial t} c_{3d} + \nabla \circ (-D_{3d} \nabla c_{3d} + \mathbf{v} c_{3d}) + \omega_{3d} c_{3d} - \theta_{3d} = f_c. \quad (13)$$

D_{3d} [cm^2/s] denotes the diffusion coefficient for oxygen in tissue. The velocity field \mathbf{v} is provided by Darcy's law:

$$\mathbf{v} = -\frac{K_{3d}}{n_{3d}} \nabla p_{3d}, \quad (14)$$

where n_{3d} denotes the porosity of the 3D tissue volume. The value ω_{3d} accounts for the tissue perfusion, i.e., it quantifies the blood flow rate from the tissue into the venous vessel system:

$$\omega_{3d} = \alpha p_{3d} - f_p = \alpha (p_{3d} - p_{ven}) - \frac{q_{out}(t)}{Vol}. \quad (15)$$

The source term f_c is given by the amount of oxygen leaving the network through the outlets of V_3 and V_4 and a Michaelis-Menten law for the metabolic rate:

$$f_c = f_c^{out} - C_{co} \cdot \frac{c_{3d}}{c_{3d,0} + c_{3d}}, \quad (16)$$

where C_{co} [$\text{mmol}/(\text{cm}^3 \text{s})$] denotes the consumption rate of oxygen in tissue and $c_{3d,0}$ [mmol/cm^3] is the average oxygen concentration in tissue. Furthermore f_c^{out} is given by:

$$f_c^{out} = \frac{Q_3^{out} \cdot \Gamma_3^{out}}{Vol \cdot A_3^{out}} \delta_{\Lambda_3(l_3)} + \frac{Q_4^{out} \cdot \Gamma_4^{out}}{Vol \cdot A_4^{out}} \delta_{\Lambda_4(l_4)},$$

where Γ_3^{out} , Γ_4^{out} , A_3^{out} and A_4^{out} are provided by the 1D models at the outlets of V_3 and V_4 . θ_{3d} is defined as follows:

$$\theta_{3d}(c_{3d}, \Gamma_i, A_i)(s) = 2\pi R_i L_{c,i} \left(\frac{\Gamma_i}{A_i}(s) - \overline{c_{3d}(s)} \right) \delta_{\Lambda_i}$$

$$\overline{c_{3d}(s)} = \int_0^1 c_{3d}(s, R_i, 2\pi\theta) d\theta, \text{ if } s \in [0, l_i], i \in \{1, \dots, 4\}. \quad (17)$$

It can be considered as a penalization term to weakly enforce the condition $\frac{\Gamma_i}{A_i} = \overline{c_{3d}}$. The average values $\overline{c_{3d}}$ are computed analogous to the average values concerning the pressure (12). $\Gamma_i/A_i = \overline{c_{3d}}$ means that the cross-sectional concentration at the actual vessel surface equals the vessel concentration Γ_i/A_i . This is the case, if the blood flow leakage term ϕ is positive, which is our hypothesis. In general one has to check, if $\phi > 0$ holds to treat A_i as a source for the tissue matrix. The parameter $L_{c,i}$ [cm s⁻¹] accounts for the permeability of the wall of vessel V_i . As boundary and initial conditions for the **Tissue perfusion** and **Transport problem**, we choose:

$$\mathcal{K}_{3d} \frac{\partial p_{3d}}{\partial \mathbf{n}} = 0, \quad \frac{\partial c_{3d}}{\partial \mathbf{n}} = 0, \quad t > 0, \quad \mathbf{x} \in \partial\Omega, \quad p_{3d}(\mathbf{x}, 0) \equiv 0, \quad c_{3d}(\mathbf{x}, 0) \equiv 0, \quad \mathbf{x} \in \Omega,$$

where \mathbf{n} is the outer normal in $\mathbf{x} \in \partial\Omega$. By these boundary conditions we enforce that there is no flux across the skin and other interfaces.

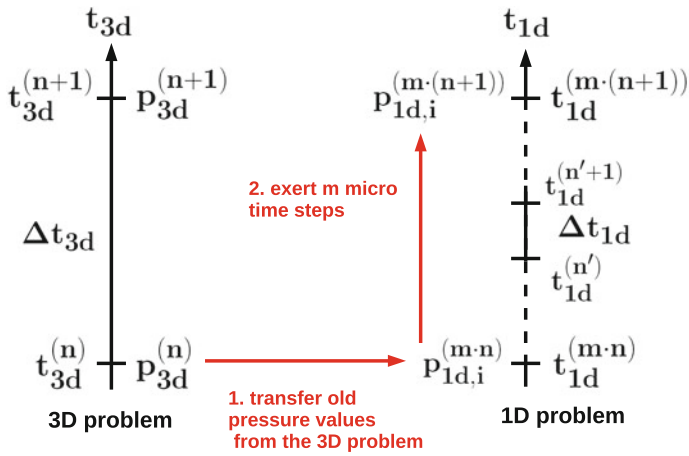
3 Numerical Discretization

The numerical solution of the 3D-1D coupled problems (10) and (13) is computed by multiple time-stepping schemes [2, 11]. These schemes have been introduced for time dependent problems in which partitioning into in slow and fast variables is meaningful. As we already pointed out in the introduction (see Sect. 1), flow and oxygen transport in the arteries is fast compared to flow and oxygen transport in the tissue. Capturing the fast wave propagation within the 1D network, small time steps are required to resolve it. On the other hand it is desirable to exert large time steps for the computational expensive 3D problems.

As a time stepping method for the 1D transport equation systems, we use the third order SSP Runge Kutta scheme [12] which is *total variational diminishing* (TVD). However, it requires a time step restriction which is at least as strict as the one for the forward Euler method. This property is no drawback in this context, because small time steps are needed for the fast flow and transport. Furthermore one time step for the 1D problems cause no great computational effort compared to the 3D problems. For the space discretization, higher order *discontinuous Galerkin* (DG) methods are applied. In the vicinity of steep gradients or discontinuities, the numerical solution is stabilized by hierarchical slope limiter techniques [16, 17].

Since the backward Euler scheme is unconditionally stable concerning the choice of the time step size, we use this scheme for the time integration in 3D. The spatial discretization is based on cell centered Finite Volumes which are robust and incorporate the conservation of mass. The 3D and 1D problems are coupled by a multiple time stepping scheme algorithm (see Fig. 3). Concerning the 3D time step

Phase 1



Phase 2

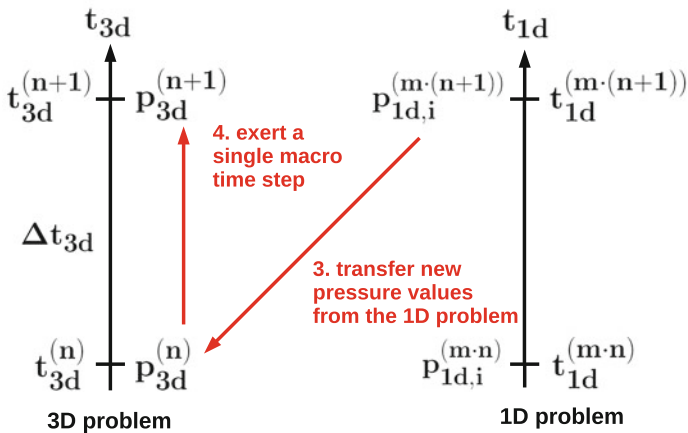


Fig. 3 Multiple time stepping scheme for the tissue perfusion problem. The transport problem can be treated in the same manner

$[t_{3d}^{(n)}, t_{3d}^{(n+1)}]$ we have the following two phases:

1. We exert m micro-steps of step size Δt_{1d} of the 1D network problem, where we use for every sub step the last computed 3D solution.
2. We advance by one macro-step of the 3D problem (step size Δt_{3d}), using the last computed 1D solution.

For our simulations we use $m = 100$.

4 Results and Discussion

Using the numerical model developed in the previous sections, we present in this section some simulation results on the influence of an arterial stenosis in a leg artery (artery 54, **right posterior tibial artery**). The degree of the stenosis is varied between 0 %, 90 % and 100 %. For 0 % and 90 % we set A_s in (9) to A_0 and $0.1 \cdot A_0$, respectively. In the case of an occlusion (stenosis degree 100 %), we set the ingoing characteristic $W_{1,54}$ at the outlet of the distal part of artery 54 to the negative value of the outgoing characteristic, i.e.: $W_{1,54} = -W_{2,54}$. By this, a full reflection at the stenosis is simulated. The computational domain for the porous matrix Ω is given by: $\Omega = 15 \times 15 \times 50$ cm.

In the following Tables 1 and 2, several parameter values and some additional information concerning the vessels V_1 - V_4 can be found. The mid axes A_i are given by cubic splines through the coordinates, where the tangents of the splines at the beginning and the end of the spline are equal to the provided tangents. The coordinates and tangents are listed in Table 3.

The different lengths, radii and the remaining vessel parameters are provided in [20, 22, Table 1]. For the simulation time we consider a period of 20 s.

Table 1 List of the fluid parameters, Poisson ratio and porous media parameters for (10) and (13)

Physical parameter	Sign	Value	Unit
Blood density	ρ	1.028	g/cm ³
Blood viscosity	η	4.500	mPa s
Poisson ratio	ν	0.500	–
Compliance	C_{3d}	0.01	kPa ⁻¹
Hydraulic permeability	K_{3d}	0.1	cm ² kPa ⁻¹ s ⁻¹
Hydraulic conductance	α	$9.4 \cdot 10^{-4}$	kPa ⁻¹ s ⁻¹
Venous pressure	p_{ven}	5.0	mmHg
Porosity	n_b	0.02	–
Diffusivity	D_{3d}	$1.7 \cdot 10^{-5}$	cm ² s ⁻¹
Consumption rate	C_{co}	0.08	$\mu\text{mol cm}^{-3} \text{s}^{-1}$
Average concentration	$c_{3d,0}$	0.72	$\mu\text{mol cm}^{-3}$

Table 2 Parameters for the subnetwork in the porous medium

Vessel	V_1	V_2	V_3	V_4
Length l_i [cm]	14.4	14.6	14.6	34.4
Radius R_i [cm]	0.361	0.375	0.375	0.197
Permeability $L_{c,i}$ [cm s ⁻¹]	10.0	10.0	10.0	10.0
Permeability $L_{p,i}$ [cm kPa ⁻¹ s ⁻¹]	0.114	0.114	0.114	0.114

The values for $L_{p,i}$ are adapted from [6, Sect. 6.6.4]

Table 3 Coordinates and tangents for the lines/mid axes A_i

A_1	Coordinates: $(7.5, 7.5, 50.0)^T$, $(4.5, 7.5, 42.0)^T$, $(3.5, 7.5, 36.8)^T$ Tangents: $(0.0, 0.0, -1.0)^T$, $(0.0, 0.0, -1.0)^T$
A_2	Coordinates: $(3.5, 7.5, 36.8)^T$, $(5.5, 5.0, 29.0)^T$, $(6.0, 4.5, 21.0)^T$, $(6.5, 4.0, 19.0)^T$ Tangents: $(-1.0, 0.0, -3.0)^T$, $(0.0, 0.0, -1.0)^T$
A_3	Coordinates: $(6.5, 4.0, 19.0)^T$, $(7.0, 3.0, 11.0)^T$, $(7.5, 2.0, 3.0)^T$ Tangents: $(0.0, 0.0, -1.0)^T$, $(0.0, 0.0, -1.0)^T$
A_4	Coordinates: $(3.5, 7.5, 36.8)^T$, $(2.5, 7.5, 28.5)^T$, $(2.0, 7.5, 20.0)^T$, $(2.5, 7.5, 11.5)^T$, $(2.8, 7.5, 3.0)^T$ Tangents: $(1.0, 0.0, -2.0)^T$, $(0.0, 0.0, -1.0)^T$

The remaining part of this section contains some simulation results concerning the described scenario. The concentration values, flow rates and pressure values are reported in the middle of all vessels, for all the narrowing degrees: 0%, 95%, 100%. To illustrate the impact of the stenosis within the peripheral artery 54, we compute the ratio between the normal condition (0%) and the other narrowing degrees. For an physiologist these values can be used to estimate the risk of an aneurysm caused by an increased pressure in a certain vessel. An aneurysm is a localized, blood filled balloon-like bulge in the wall of a blood vessel [3]. As an aneurysm grows, the risk of rupture becomes higher and higher. When it is torn apart, it can lead to bleeding and a subsequent hypovolemic shock leading to death.

The relative values of the quantities for the embedded subnetwork can be seen in Fig. 4. Clearly, the pressure and the flow rate break down in Vessel 3 beyond the stenosis. Considering the same physical values within the other embedded vessels, one can observe that the pressure is remarkably increased (up to 37.0% for an occlusion). If the walls of these vessels are weakened at a certain location, there is a high risk that an aneurysm is formed. The flow rates in the feeding vessels V_1 and V_2 are decreased. This blood flow reduction leads to an insufficient blood and oxygen supply of the tissue (see Fig. 5). Apparently this reduction can not be compensated by the increased flow rate (up to 27.0% for an occlusion) within vessel V_4 . Due to the stabilization techniques for the 1D discretization and the robust Finite Volume discretization for the 3D problem there are neither for the 3D problem nor for the 1D problem unphysical oscillations around the concentration fronts. Behind the concentration front in 3D, the concentration values range from 0.0070 to 0.0074 mmol/cm³. This is in agreement with other literature [6, Sect. 6.6], in which the value 0.0072 mmol/cm³ was taken as a reference value for blood oxygen concentration in tissue.

However the propagation speed of the concentration front is too slow, and the pressure values within the porous matrix are too low compared to other literature [6, Sect. 6.6]. Figure 6 shows the pressure values within the cross section at $y = 7.5$ cm and at certain time points. To compute a more realistic propagation of the oxygen concentration and pressure values, a better estimation of the involved

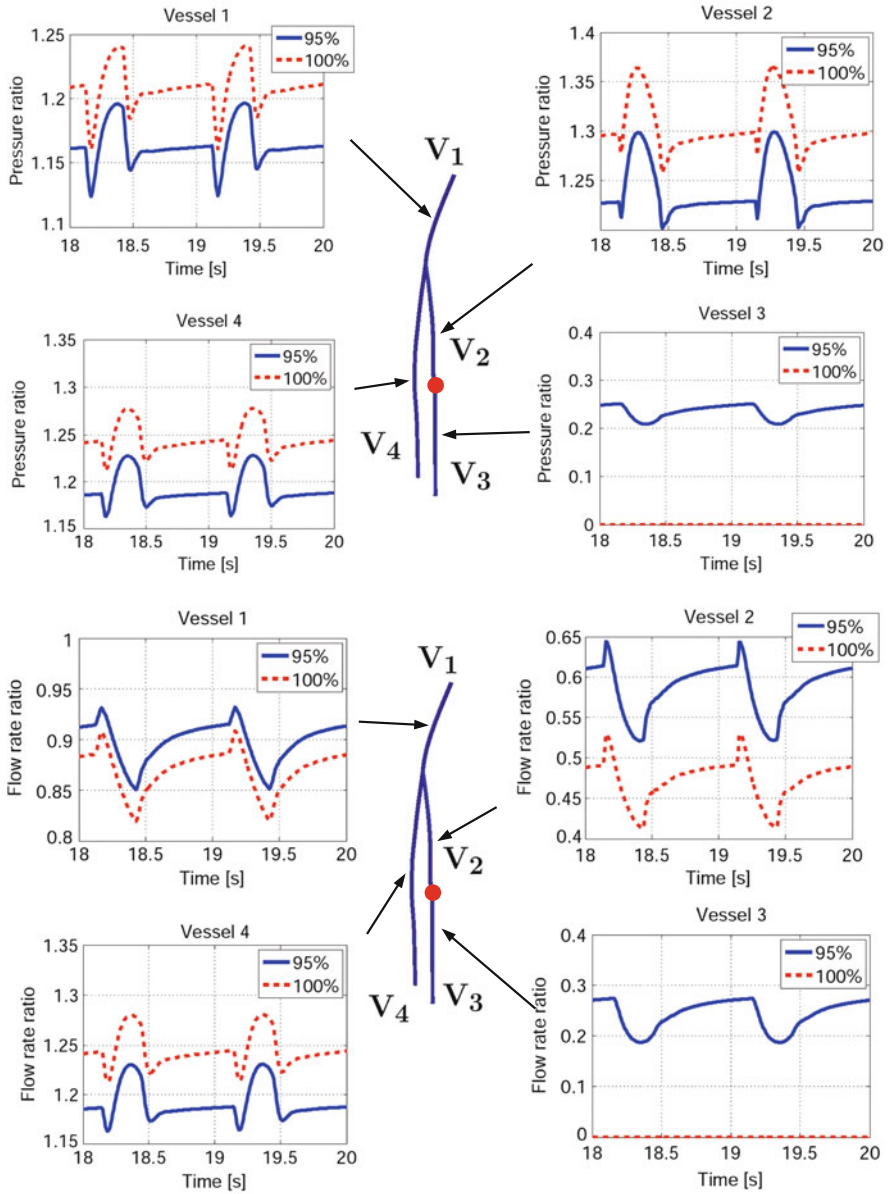


Fig. 4 Pressure and flow rate ratios within the embedded vessels. The ratios are computed by comparing the abnormal states (95 %, 100 % narrowing) to the healthy state (0 % narrowing)

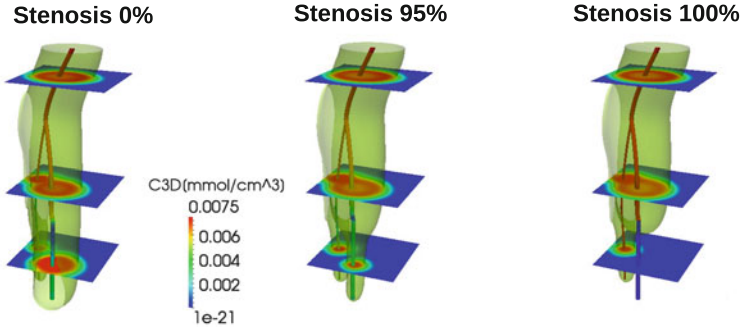


Fig. 5 Oxygen concentration distribution c_{3d} (at $t = 20$ s) within three different slices at $z = 45$, $z = 25$ and $z = 10$ and for different narrowing factors: 0%, 95% and 100%. The concentration front corresponds to the value 0.005 mmol/cm^3

parameters combined with a hierarchical model for flow and transport within the porous medium is required [21].

5 Conclusion

In this paper, we have presented a 3D-1D-0D coupled multi-scale model to simulate the local impact of a peripheral stenosis on local blood perfusion and oxygen supply. Transport and flow in the 3D tissue have been modeled by standard porous medium equations whereas the 1D models are given by transport equation systems. Lumped parameter models have been used to simulate the stenosis and the omitted vessels. The 3D and 1D system have been coupled by its source terms, where the 1D problems are embedded into the 3D matrix by Dirac line measures. For the numerical solution multiple time stepping schemes have been considered. The 3D problems have been solved by Finite Volume schemes, for the 1D problems stabilized DG methods have been used. It has been revealed that the pressures in the vessels in front of the stenosis are remarkably increased which may lead to an aneurysm in this area. The reduced blood perfusion and oxygen supply in the tissue can be clearly observed. However, the propagation of the concentration front is too slow and the pressure are too low. This could be improved by a better estimation of the porous medium parameters and a hierarchical flow model within the tissue [21].

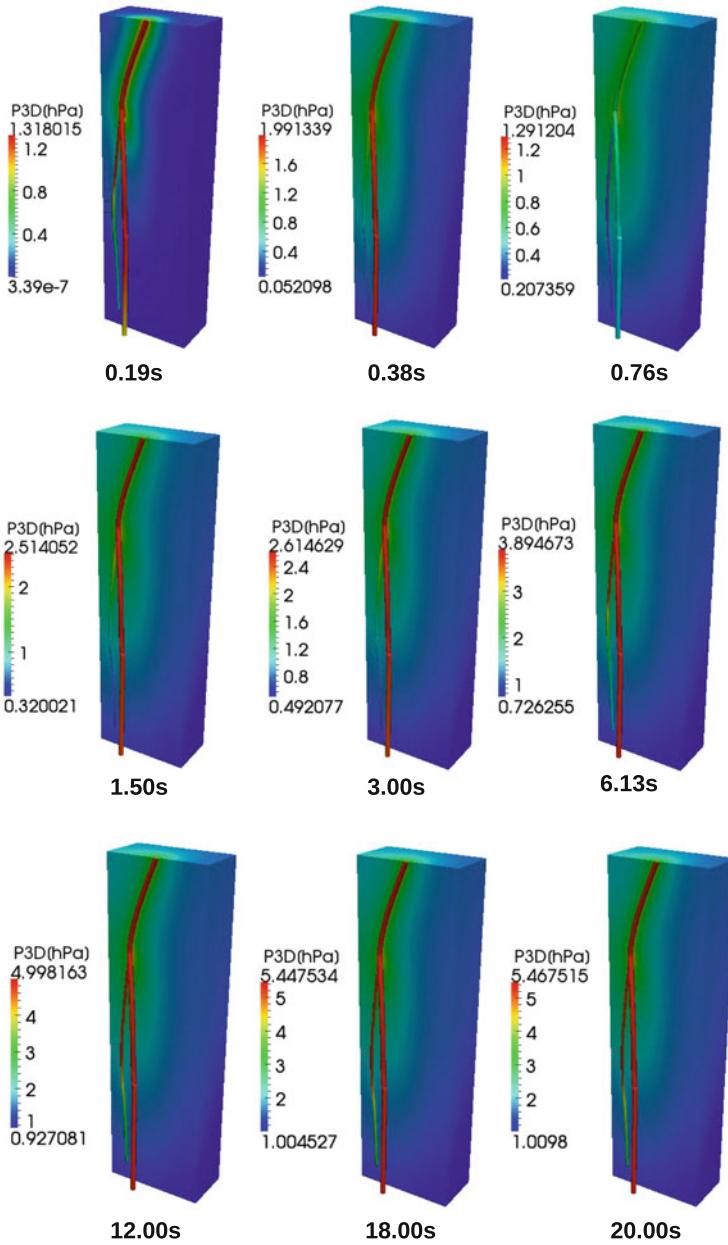


Fig. 6 Snapshots of the pressure distribution p_{3d} . The cross section is placed at $y = 7.5$ cm

References

1. Alastruey, J., Parker, K., Peiro, J., Sherwin, S.: Lumped parameter outflow models for 1-D blood flow simulations: effect on pulse waves and parameter estimation. *Commun. Comput. Phys.* **4**, 317–336 (2008)
2. Andrus, J.F.: Numerical solution of systems of ordinary differential equations separated into subsystems. *SIAM J. Numer. Anal.* **16**(4), 605–611 (1979)
3. Behrends, J., Bischofberger, J., et. al.: *Duale Reihe Physiologie*, 2nd. Auflage. Thieme Verlag, Stuttgart (2012)
4. Canic, S., Kim, E.: Mathematical analysis of quasilinear effects in a hyperbolic model blood flow through compliant axi-symmetric vessels. *Math. Methods Appl. Sci.* **26**, 1161–1186 (2003)
5. Cattaneo, L., Zunino, P.: Computational models for fluid exchange between microcirculation and tissue interstitium. *Netw. Heterog. Media* **9**, 135–159 (2014)
6. D’Angelo, C.: Multiscale modelling of metabolism and transport phenomena in living tissues. Ph.D. thesis, EPFL, Lausanne (2007)
7. D’Angelo, C., Quarteroni, A.: On the coupling of 1D and 3D diffusion-reaction equations. Applications to tissue perfusion problems. *Math. Models Methods Appl. Sci.* **18**(8), 1481–1504 (2008)
8. Erbertseder, K.M.: A multi-scale model for describing cancer-therapeutic transport in the human lung. Ph.D. thesis, University of Stuttgart (2012)
9. Formaggia, L., Nobile, F., Veneziani, A., Quarteroni, A.: Multiscale modelling of the circulatory system: a preliminary analysis. *Vis. Sci.* **2**, 75–83 (1999)
10. Formaggia, L., Quarteroni, A., Veneziani, A.: *Cardiovascular mathematics-modelling and simulation of the circulatory system*. Springer, Italia, Milano (2009)
11. Gear, C., Wells, D.: Multirate linear multistep methods. *BIT* **24**(4), 484–502 (1984)
12. Gottlieb, S., Shu, C.W.: Total variation diminishing Runge-Kutta schemes. *Math. Comput.* **67**, 73–85 (1998)
13. Khaled, A.R.A., Vafai, K.: The role of porous media in modeling flow and heat transfer in biological tissues. *Int. J. Heat Mass Transf.* **46**(26), 4989–5003 (2003)
14. Koepl, T., Wohlmuth, B., Helmig, R.: Reduced one-dimensional modelling and numerical simulation for mass transport in fluids. *Int. J. Numer. Methods Fluids* **72**(2), 135–156 (2013)
15. Koepl, T., Schneider, M., Pohl, U., Wohlmuth, B.: The influence of an unilateral carotid artery stenosis on brain oxygenation. *Med. Eng. Phys.* **36**(7), 905–914 (2014)
16. Krivodovona, L.: Limiters for high-order discontinuous Galerkin methods. *J. Comput. Phys.* **226**, 879–896 (2007)
17. Kuzmin, D.: A vertex-based hierarchical slope limiter for p-adaptive discontinuous Galerkin methods. *J. Comput. Appl. Math.* **233**, 3077–3085 (2010)
18. Schmidt, R., Lang, F., Heckmann, M.: *Human Physiology, Second Completely, Revised Edition*. Springer, Berlin, Heidelberg, New York (1989)
19. Sherwin, S., Franke, V., Peiro, J., Parker, K.: One-dimensional modelling of a vascular network in space-time variables. *J. Eng. Math.* **47**, 217–250 (2003)
20. Stergiopoulos, N., Young, D., Rogge, T.: Computer simulation of arterial flow with applications to arterial and aortic stenoses. *J. Biomech.* **25**, 1477–1488 (1992)
21. Vankan, W., Huyghe, J.M., Janssen, J., Huson, A., Hacking, W., Schreiner, W.: Finite element analysis of blood perfusion through biological tissue. *Int. J. Eng. Sci.* **35**, 375–385 (1997)
22. Wang, J., Parker, K.: Wave propagation in a model of the arterial circulation. *J. Biomech.* **37**, 457–470 (2004)